

**Relativistic electron-atom scattering in an extremely powerful laser field: Relevance of spin effects**

P. Panek and J. Z. Kamiński

*Institute of Theoretical Physics, Warsaw University, Hoża 69, 00681 Warszawa, Poland*

F. Ehlotzky\*

*Institute for Theoretical Physics, University of Innsbruck, Technikerstrasse 25, A-6020 Innsbruck, Austria*

(Received 14 June 2001; published 8 February 2002)

We reconsider the relativistic scattering of electrons by an atom, being approximated by a static potential, in an extremely powerful electromagnetic plane wave of frequency  $\omega$  and linear polarization  $\varepsilon$ . Since to a first order of approximation spin effects can be neglected, we first describe the scattered electron by the Gordon solution of the Klein-Gordon equation. Then we investigate the same scattering process by including the spin effects, using for the electron the Volkov solution of the Dirac equation. For sufficiently energetic electrons, the first-order Born approximation can be employed to represent the corresponding scattering matrix element. We compare the results of the differential cross sections of induced and inverse bremsstrahlung, evaluated from both approximations, for various parameter values and angular configurations and we find that in most cases the spin effects are marginal, even at very high laser power. On the other hand, we recover the various asymmetries in the angular distributions of the scattered electrons and their respective energies due to the laser-induced drift motion of the electrons in the direction of propagation of the radiation field, thus confirming the findings of our previous work [Phys. Rev. A **59**, 2105 (1999); Laser Physics **10**, 163 (2000)].

DOI: 10.1103/PhysRevA.65.033408

PACS number(s): 34.50.Rk, 34.80.Qb, 32.80.Wr

**I. INTRODUCTION**

Soon after the invention of the laser, two basic quantum processes were thoroughly investigated with emphasis on the laser-induced nonlinearities. The first of them was laser-induced Compton scattering and the second was laser-modified electron-atom scattering. A nice discussion of the early work on the first of these processes can be found in the review by Eberly [1]. The original work on free-free transitions in a powerful laser field is clearly summarized in the overview by Bunkin *et al.* [2]. More elaborate introductions into this field of research can be found in the books by Mittleman [3] and by Faisal [4] and summaries of more recent work are presented in several reviews [5–9]. With the advent of very powerful laser sources, yielding intensities of  $10^{18}$  W cm $^{-2}$  and above, it has become important to consider laser-modified and laser-induced processes relativistically [10,11]. Hence, Mott scattering in a powerful, circularly polarized radiation field was reconsidered very recently by Szymanowski *et al.* [12] with reference to much earlier investigations of this process [13–25]. By evaluating the nonlinear cross sections numerically, large relativistic corrections were found by these authors, if their data are compared with the results of the Bunkin-Fedorov [26] or Kroll-Watson [27] formulas. On the other hand, this work appears to have shown that electron-spin effects become relevant only if the laser intensity is such that the critical parameter  $\mu = |e|F_0/m\omega c$  comes close to unity. In this parameter  $e$  is the electric charge,  $F_0$  is the electric-field strength,  $m$  is the electron mass,  $\omega$  is the laser frequency, and  $c$  is the speed of light. For a Nd:YAG Yttrium aluminum garnet laser the value of  $\mu \approx 1$  corresponds to a laser-field intensity of the

order of magnitude mentioned above. For somewhat lower field intensities, it was found in the above work that spin effects are negligible and instead of using the Volkov solution of the Dirac equation [28] for describing an electron embedded in the laser field, one may safely use the corresponding Gordon solution [29] of the Klein-Gordon equation. To simplify their calculations, Szymanowski *et al.* [12] considered electron scattering in a powerful circularly polarized laser field. The scattering process in this configuration is, however, not so effective and rich in details as in the case of linear polarization, as we were able to show in our earlier semirelativistic and relativistic work on this problem, neglecting in a first-order approximation the effects of the electron spin [30–32]. Apparently, for linearly polarized laser light the oscillating electron will encounter more often the target atom during the scattering process and therefore the laser-modified collision process will, in the relativistic case, be much more effective and richer in its angular and polarization dependences than for circular laser polarization, as we discussed in our earlier work [31]. It is the purpose of the present work to reanalyze all these effects in more detail, in particular, for a very powerful, linearly polarized laser field, and to compare the results of relativistic calculations for Bose and Dirac particles to find out the relevance of spin effects at very high laser-field strength, and to investigate whether effects can be encountered that are strong enough to be accessible to observation in the relativistic regime.

During the investigation of laser-induced Compton scattering [1], a laser-induced electron drift motion and, consequently, an intensity-dependent frequency shift of the Compton light was predicted. This shift is proportional to  $\mu^2$  and was very small for the available laser intensities in the early days of laser research. One of the present authors was therefore looking for a process that would more easily permit to observe the effect of the laser-induced drift motion of the

\*Email address: Fritz.Ehlotzky@uibk.ac.at

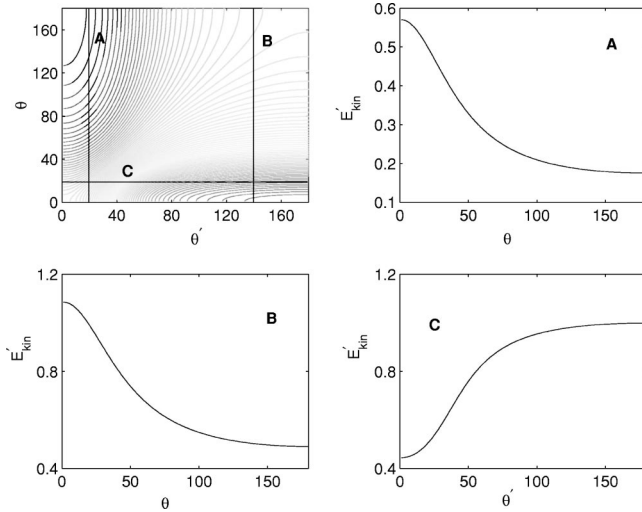


FIG. 1. The upper left panel shows a contour plot of the final kinetic electron energies  $E'_{kin}$ , measured in units of the electron's rest-energy  $m$ , as a function of  $\theta$  and  $\theta'$  and in the panels (A), (B), and (C) these energies are presented for the cuts A, B, and C indicated in the contour plot. The initial kinetic energy is  $E_{kin} = 0.5 m$ , the laser intensity  $I = 1.28 \times 10^{18} \text{ W cm}^{-2}$  ( $\mu = 1$ ), the laser frequency  $\omega = 1.17 \text{ eV}$ , and the number of absorbed photons  $N = 10^3$ .

electron. Considering in a semirelativistic approximation, potential scattering of electrons in a laser field, he found in the low-frequency limit the following asymmetry in the total laser-assisted differential scattering cross sections [33]:

$$\frac{d\sigma^{(-)} - d\sigma^{(+)}}{d\sigma^{(-)} + d\sigma^{(+)}} \approx \frac{\mu^2}{2\beta} \sin \theta. \quad (1)$$

$\mu^2$  is related to the electron drift velocity in the laser field by the relation  $v_d = \mu^2 c$  and  $\beta = v/c$  where  $v$  is the velocity of the scattered electron.  $\theta$  denotes the scattering angle. The scattering configuration considered, leading to the above asymmetry relation, was depicted in Fig. 1 of [30] in which the scattering plane is determined by the vector  $\epsilon$  of linear polarization of the laser beam and by the direction  $\mathbf{n}$  of its propagation. The momentum  $\mathbf{p}$  of the ingoing electrons is oriented parallel to  $\epsilon$  and the momentum  $\mathbf{p}'$  of the outgoing electrons can be either in the direction denoted by  $(-)$ , having an angle  $\pi/2 + \theta$  with the direction  $\mathbf{n}$ , or in the direction  $(+)$  with an angle  $\pi/2 - \theta$  with respect to  $\mathbf{n}$ . Even though the laser-induced effect is here proportional to  $\mu^2/\beta$  and not like the Compton-drift effect proportional to  $\mu^2$ , at the time of writing the above paper, laser powers and thus  $\mu^2$  were still much too low and therefore the process remained of little interest. Nowadays the experimental situation has drastically changed and the electron's drift motion in a powerful laser field has been verified experimentally [10] and thus the above effect appeared to be accessible to experimental verification. But we were able to show in our preceding investigations [30–32] that actually such asymmetries are much more complicated and that in the same semirelativistic approximation a similar asymmetry relation, as Eq. (1), can be

derived for the observed electron kinetic energies in the direction  $(+)$  and  $(-)$ , respectively, namely,

$$\frac{\Delta E'_{kin}}{2E_{kin}} = \frac{\mu^2}{2\beta} \sin \theta, \quad (2)$$

where  $\Delta E'_{kin} = E_{kin}^{(-)} - E_{kin}^{(+)}$  is evaluated from  $E'_{kin} = E_{kin} - (\mu^2/4)(\mathbf{p}' - \mathbf{p}) \cdot \mathbf{n} + N\omega$  with  $N$  being the number of emitted or absorbed laser photons. The above asymmetry relation, Eq. (2), for the observed electron energies is more reasonably well fulfilled in exact relativistic calculations.

In order to show that spin effects in the present process should be rather marginal, we shall perform the following quasiclassical consideration. We start from the Dirac equation, in its quadratic form, for a particle in an electromagnetic field, which can be found in Schiff's book on quantum mechanics [34] (using throughout this paper units  $\hbar = c = 1$ ),

$$[(E - e\phi)^2 - m^2]\psi = [(\mathbf{p} - e\mathbf{A})^2 - e\sigma' \cdot \mathbf{B} + ie\alpha \mathbf{E}] \psi, \quad (3)$$

in which  $\mathbf{A}$  and  $\phi$  are the electromagnetic potentials while  $\mathbf{E}$  and  $\mathbf{B}$  are the electric- and magnetic-field strengths, respectively.  $\sigma'$  and  $\alpha$  are Dirac's spin matrices. Considering an electromagnetic, linearly polarized plane wave of frequency  $\omega$ , unit vector of polarization  $\epsilon = \mathbf{e}_y$ , and direction of propagation  $\mathbf{n} = \mathbf{e}_x$  in the Coulomb gauge,  $\mathbf{A} = A_0 \mathbf{e}_y \cos \omega(t-x)$  and  $\phi = 0$ , we can infer from Eq. (3) a semiclassical expression for the final kinetic energy  $E'_{kin} = E' - m$  of an electron placed into this field with initial momentum  $\mathbf{p}$  along the  $y$  axis. Since  $\mathbf{E}$  points along the  $y$  axis,  $\mathbf{B}$  will point into the  $z$  direction. Therefore the magnetic term in Eq. (3) can be replaced by  $-eA_0\omega\sigma'_z \sin \omega(t-x)$  and the electric term by  $ieA_0\omega\alpha_y \sin \omega(t-x)$ . For  $\sigma'_z$  we can take in our quasiclassical calculation the two values  $\pm 1$ , while  $\alpha_y$  couples in a matrix element the two large components of a Dirac spinor with the two small components and therefore we have to take  $\pm ip/(E+m)$ , where the initial energy is  $E = E_{kin} + m$ . Therefore we obtain from Eq. (3)

$$\begin{aligned} E'_{kin} \left( 1 + \frac{E'_{kin}}{2m} \right) &= E_{kin} \left( 1 + \frac{E_{kin}}{2m} \right) \\ &\quad - 2 \sqrt{2E_{kin} \left( 1 + \frac{E_{kin}}{2m} \right)} U_p \cos \omega(t-x) \\ &\quad + U_p [1 + \cos 2\omega(t-x)] \\ &\quad \mp \sqrt{\frac{U_p}{m}} \omega \left[ 1 + \sqrt{\frac{E_{kin}}{E_{kin} + 2m}} \right] \sin \omega(t-x). \end{aligned} \quad (4)$$

From this expression we obtain the maximum electron kinetic energy  $E_{kin}^{\max}$  in the laser field with maximum spin contribution, if we choose the radiation phase to be  $\omega(t-x) = \pi/4$  or  $3\pi/4$  in which case  $\sin \omega(t-x) = \pm 1/\sqrt{2}$  and  $\cos 2\omega(t-x) = 0$ . With this choice we find

$$E_{kin}^{\max} \left( 1 + \frac{E_{kin}^{\max}}{2m} \right) = E_{kin} \left( 1 + \frac{E_{kin}}{2m} \right) + U_p \pm \frac{\omega}{\sqrt{2}} \sqrt{\frac{U_p}{m}} \left[ 1 + \sqrt{\frac{E_{kin}}{E_{kin} + 2m}} \right], \quad (5)$$

where  $E_{kin}$  is the initial kinetic energy of the electron entering the radiation field.  $U_p = m\mu^2/4$  is the ponderomotive energy of the electron in the laser field with  $\mu$  being the intensity parameter defined above. The formula (5) immediately tells us that for laser-field intensities in the relativistic regime, i.e., for  $\mu = 1$  and thus  $U_p = m/4$ , the ratio between laser-induced spin effects and laser-induced dynamical effects will be  $2\omega/m \simeq 10^{-6}$  for a Nd:YAG laser with  $\omega = 1.17$  eV. Consequently, on the basis of these quasiclassical considerations, the spin effects in the potential scattering of electrons in a very powerful laser field should be marginal. It is also interesting to remark that according to Eq. (4) the contributions of the laser-induced spin effects and of the laser-induced dynamical effects are out of phase by  $\pi/2$  in their influence on the total final energy of the electron in the field. Moreover, we recognize that for relativistic initial electron kinetic energies,  $E_{kin} = m$ , the electric spin term in Eq. (3) will contribute in the square brackets of the last term of Eq. (5) a factor  $\sqrt{1/3}$ , showing that also in the relativistic case the magnetic-spin term yields the dominant contribution. On the other hand, for lower laser intensities we usually have  $U_p \ll E_{kin}$  and  $\mu \ll 1$  so that in this case the relevant ratio is  $\omega\mu/2E_{kin} \ll 1$  and therefore also in the nonrelativistic regime spin effects are negligible. Our numerical results, presented below, will confirm the findings of these heuristic considerations.

## II. RELATIVISTIC CROSS-SECTION FORMULAS

### A. Scattering of a Klein-Gordon particle

In our earlier work [30–32] the laser-dressed electron was described by the Gordon solution [29] of the Klein-Gordon equation and the scattering process was described in the first-order Born approximation using as target a screened Coulomb potential. Since in the following investigation we shall consider electron scattering in the relativistic region of the laser-field intensity and of the electron kinetic energy, the first-order Born approximation should be sufficiently accurate and we can take over the main results from our work quoted before. We derived the exact solution of the Klein-Gordon equation for a particle of mass  $m$  and charge  $e$  placed into an electromagnetic plane-wave field, described by the vector potential  $\mathbf{A}(\tau)$  in the Coulomb gauge, where  $\tau = t - \mathbf{n} \cdot \mathbf{x}$  and  $\mathbf{n}$  is the direction of propagation of the field. In case the powerful laser field is approximately described by a monochromatic plane wave of amplitude  $A_0 = F_0/\omega$ , linear polarization  $\epsilon$ , frequency  $\omega$ , and wave vector  $\mathbf{k} = k\mathbf{n}$ , the vector potential reads

$$\mathbf{A}(\tau) = A_0 \epsilon \cos \omega \tau \quad (6)$$

and for a particle of initial energy  $E$  and momentum  $\mathbf{p}$ , as-

suming adiabatic decoupling of the particle from the field at  $t \rightarrow -\infty$ , the Gordon solution, normalized to the volume  $V$ , has then the form [35]

$$\psi_{\mathbf{p}} = (2EV)^{-1/2} \exp[-i(\bar{E}t - \bar{\mathbf{p}} \cdot \mathbf{r})] \exp[ia \sin \omega \tau - b \sin 2\omega \tau], \quad (7)$$

where in this expression the following abbreviations have been introduced:

$$\bar{E} = E + d, \bar{\mathbf{p}} = \mathbf{p} + d\mathbf{n}, d = \frac{m^2 \mu^2/4}{E - \mathbf{p} \cdot \mathbf{n}},$$

$$a = \frac{m(\mu/k)\mathbf{p} \cdot \epsilon}{E - \mathbf{p} \cdot \mathbf{n}}, b = \frac{m^2 \mu^2/8\omega}{E - \mathbf{p} \cdot \mathbf{n}}, \mu^2 = (eA_0/m)^2. \quad (8)$$

The renormalized energy  $\bar{E}$  and momentum  $\bar{\mathbf{p}}$  fulfill the conservation relation  $\bar{E}^2 = \bar{m}^2 + \bar{\mathbf{p}}^2$ , which corresponds to an on-shell particle of effective mass  $\bar{m} = m(1 + \mu^2/2)^{1/2}$  [36]. The characteristic intensity parameter, introduced in the Introduction, is given by  $\mu^2 = I/I_c$ , where  $I$  is the average intensity of the laser radiation and  $I_c = \alpha\omega^2/8\pi r_0^2$  ( $\alpha = e^2, r_0 = e^2/m$ ) is the critical laser intensity at which  $\mu^2 = 1$  in which case the problem has to be treated relativistically. Similarly, we can find the wave function  $\psi_{\mathbf{p}'}^*$ , which describes the scattered electron of energy  $E'$  and momentum  $\mathbf{p}'$  with the corresponding coefficients  $a', b'$ , and  $d'$  like in Eq. (8). Then we obtain from the first-order Born approximation, using for the scattering potential  $U(\mathbf{r})$  a screened Coulomb potential of charge  $eZ$  and screening length  $\ell$ , in a straightforward manner the differential cross sections of the laser-induced nonlinear bremsstrahlung processes,

$$d\sigma_N = \frac{(e^2 Z)^2 (\bar{E}'_N + \bar{E})^2 d\Omega'}{[(\bar{\mathbf{p}}' - \bar{\mathbf{p}} - N\mathbf{k})^2 + \ell^{-2}]^2} \frac{p'_N}{p F_N} M_N^2, \quad (9)$$

where scattering takes place into the solid angle  $d\Omega'$  and the energy conservation relation reads for these processes

$$\bar{E}'_N = \bar{E} + N\omega \quad \bar{p}'_N = (\bar{E}'_N^2 - \bar{m}^2)^{1/2}. \quad (10)$$

The factor  $F_N$  that appears in the denominator of the cross-section formula (9) has the form

$$F_N = 1 - \frac{d'_N}{E'_N - \mathbf{p}'_N \cdot \mathbf{n}} \left( 1 - \frac{E'_N \mathbf{p}'_N \cdot \mathbf{n}}{p'^2_N} \right). \quad (11)$$

Moreover, the matrix elements  $M_N$  are found to be

$$M_N = B_N(x, y) - \frac{\omega(a' + a)}{2(\bar{E}' + \bar{E})} [B_{N+1}(x, y) + B_{N-1}(x, y)] + \frac{\omega(b' + b)}{\bar{E}' + \bar{E}} [B_{N+2}(x, y) + B_{N-2}(x, y)]. \quad (12)$$

In this expression we have introduced the following generalized Bessel functions:

$$B_N(x, y) = \sum_{\lambda=-\infty}^{+\infty} J_{N-2\lambda}(x) J_{\lambda}(y) \quad (13)$$

in which  $J_{N-2\lambda}(x)$  and  $J_{\lambda}(y)$  represent ordinary Bessel functions of the first kind. The coefficients  $x$  and  $y$  in these functions are defined by

$$x = a' - a, \quad y = b - b', \quad (14)$$

where  $a$  and  $b$  and similarly  $a'$  and  $b'$  are given by Eqs. (8). From the energy-conservation relation, Eq. (10), it becomes clear that all primed quantities depend on the order of nonlinearity  $N$ . In the case of low laser intensities, i.e.,  $\mu^2 \ll 1$ , and small kinetic energies, i.e.,  $(E - m)/m \ll 1$ , the expression in Eq. (9) reduces to the nonrelativistic formula of Bunkin and Fedorov [26]

$$d\sigma_N^{NR} = \frac{(2r_0 Z)^2 m^4 d\Omega'}{(\mathbf{Q}_N^2 + \ell^{-2})^2} \frac{p'_N}{p} J_N^2(\mu \mathbf{Q}_N \cdot \boldsymbol{\epsilon} / \omega), \quad (15)$$

in which  $\mathbf{Q}_N = \mathbf{p} - \mathbf{p}'_N$ . The corresponding nonrelativistic energy-conservation relation reads  $E'_{kin} = E_{kin} + N\omega$ . To these formulas we shall refer later on in our discussion of the numerical data obtained from the relativistic theories.

### B. Scattering of a Dirac particle

The evaluation of the nonlinear cross sections for the potential scattering of a Dirac electron of spin 1/2, embedded in a powerful electromagnetic plane-wave field, can proceed in a very similar manner as was done for a Klein-Gordon particle in the foregoing section. We start from the Dirac equation in an arbitrary plane-wave field,

$$(i\gamma^\mu \partial_\mu - e\gamma^\mu A_\mu - m)\psi(x) = 0, \quad (16)$$

where the vector potential  $A_\mu$  has the general form

$$A_\mu = A_\mu(k \cdot x), \quad A \cdot k = k \cdot k = 0 \quad (17)$$

and we use the Einstein summation convention and notation, namely,  $v^\mu w_\mu = v \cdot w$ , where  $\mu = 0, 1, 2, 3$ . The solution of the above Dirac equation (16) in a plane-wave field was derived by Volkov [28] and its explicit form can be found in the paper by Denisov and Fedorov [13],

$$\begin{aligned} \psi(x) = & [1 + \kappa \gamma^\mu k_\mu \gamma^\nu A_\nu(k \cdot x)] \\ & \times \exp\left[-ip \cdot x - i \int_0^{k \cdot x} S(\phi) d\phi\right] u_p, \end{aligned} \quad (18)$$

where  $u_p$  is a free-particle solution of  $(\gamma^\mu p_\mu - m)u_p = 0$  with  $p_\mu$  being a four-vector. The constant  $\kappa$  and the function  $S(\phi)$  can be evaluated and we find

$$S(\phi) = \frac{eA(\phi) \cdot p}{p \cdot k} + \frac{e^2 A^2(\phi)}{2p \cdot k}, \quad \kappa = \frac{e}{2p \cdot k}, \quad (19)$$

where  $A(\phi)$  is the four-vector of the vector potential Eq. (17). Then, after normalization to the volume  $V$ , the required Volkov solution for an electron of initial four-momentum  $p$  reads

$$\begin{aligned} \psi_p(x) = & \sqrt{\frac{m}{VE_p}} \left[ 1 - \frac{e\gamma^\mu A_\mu(k \cdot x) \gamma^\nu k_\nu}{2k \cdot p} \right] \exp\left[-ip \cdot x \right. \\ & \left. - i \int_0^{k \cdot x} \left( \frac{eA(\phi) \cdot p}{p \cdot k} + \frac{e^2 A^2(\phi)}{2p \cdot k} \right) d\phi \right] u_p. \end{aligned} \quad (20)$$

For considering Mott scattering in a powerful laser field in the first-order Born approximation we have to evaluate the  $T$ -matrix element

$$T_{fi} = -i \int dx \bar{\psi}_{p'}(x) \gamma^\mu U_\mu(x) \psi_p, \quad (21)$$

where scattering takes place for an electron of initial four-momentum  $p$  to a final momentum  $p'$ . In Eq. (21) we describe the ingoing and outgoing electron by Volkov waves of the form (20) and we decompose this matrix element into its Fourier components in space and time, using the definition of the generalized Bessel functions (13). Then we find by straightforward calculation

$$\begin{aligned} T_{fi} = & -i \frac{m}{V\sqrt{E'E}} \sum_N \int dt \exp[i(\bar{E}' - \bar{E} - N\omega)t] \\ & \times \int d\mathbf{r} U(\mathbf{r}) \exp[-i(\bar{\mathbf{p}}' - \bar{\mathbf{p}} - N\omega\mathbf{n}) \cdot \mathbf{r}] M_N, \end{aligned} \quad (22)$$

where  $U(\mathbf{r})$  is a screened Coulomb potential of charge  $eZ$  and screening length  $\ell$  and the nonlinear matrix elements  $M_N$  are given by

$$\begin{aligned} M_N = & B_N \bar{u}_{p'} \gamma^0 u_p + \frac{eA_0}{4k \cdot p'} (B_{N+1} + B_{N-1}) \bar{u}_{p'} \gamma^\mu \epsilon_\mu k^\nu \gamma_\nu \gamma^0 u_p \\ & - \frac{eA_0}{4k \cdot p} (B_{N+1} + B_{N-1}) \bar{u}_{p'} \gamma^0 \gamma^\mu \epsilon_\mu k^\nu \gamma_\nu u_p \\ & - \frac{e^2 A_0^2}{8(k \cdot p')(k \cdot p)} \left[ B_N + \frac{1}{2}(B_{N+2} + B_{N-2}) \right] \\ & \times \bar{u}_{p'} \gamma^\mu \epsilon_\mu k^\nu \gamma_\nu \gamma^0 \gamma^\sigma \epsilon_\sigma k^\tau \gamma_\tau u_p, \end{aligned} \quad (23)$$

in which we assumed the plane-wave field to be monochromatic and linearly polarized so that in the Coulomb gauge,  $A_\mu$  has the explicit form

$$\begin{aligned} A^\mu(k \cdot x) = & A_0 \epsilon^\mu \cos(k \cdot x), \quad \epsilon^\mu \equiv (0, \boldsymbol{\epsilon}), \\ & \epsilon^2 = -1, \quad \bar{\epsilon}^2 = 1. \end{aligned} \quad (24)$$

Under these conditions, in the matrix element of Eq. (23) the arguments  $x$  and  $y$ , defined in Eq. (14) of the generalized Bessel functions, are the same as those in Eq. (8) for a Klein-Gordon particle. Since the Fourier transform  $U(\mathbf{q})$  of the



screened Coulomb potential in Eq. (22) can be easily calculated, we are able to evaluate from Eq. (22) the transition probability per unit time to read

$$w_{fi} = \lim_{T \rightarrow \infty} \frac{|T_{fi}|^2}{T} = \sum_N \frac{2\pi m^2}{V^2 E' E} \times |U(\bar{\mathbf{p}}' - \bar{\mathbf{p}} - N\omega\mathbf{n})M_N|^2 \delta(\bar{E}' - \bar{E} - N\omega), \quad (25)$$

where for the laser-dressed electron momenta and energies the same notation is used as in Eq. (8) of the preceding section. From the transition probabilities, Eq. (25), we can finally evaluate the differential cross sections of the nonlinear scattering processes of the order  $N$ . We find

$$\frac{d\sigma_N^{(s,s')}}{d\Omega'} = \frac{p'_N}{p} \frac{4(mZ\alpha)^2}{F_N} \frac{|M_N|^2}{[(\bar{\mathbf{p}}' - \bar{\mathbf{p}} - N\mathbf{k})^2 + \ell^{-2}]^2}. \quad (26)$$

In this equation, the indices  $s$  and  $s'$  label the spin polarizations of the incoming and outgoing electrons and have the possible values  $+$  or  $-$ . These indices,  $\pm$ , have the meaning that the spin polarization of an electron in its rest frame has the values  $\pm 1/2$  with respect to the  $z$  axis. For an unpolarized beam of electrons, we should average over the initial and sum over the final spin polarizations, viz.,

$$\frac{d\sigma_N}{d\Omega'} = \frac{1}{2} \sum_{s,s'=\pm} \frac{d\sigma_N^{(s,s')}}{d\Omega'}. \quad (27)$$

The energy-conservation relation, which follows from Eq. (25), is the same as in Eq. (10) for scattering of a Klein-Gordon particle and the same is true for the generalized Bessel functions  $B_N$  and their arguments, defined in Eqs. (13) and (14). Similarly, we obtain in evaluating the phase space the same function  $F_N$  defined in Eq. (11). The evaluation of the matrix elements, appearing in the Eq. (23) and containing Dirac spinors and  $\gamma$  matrices, is performed numerically and therefore their explicit result will not be written down here. In the following section we shall present a comparison of the cross sections calculated for scattering of a spin-0 or a spin-(1/2) particle in a very powerful laser field and we shall see that spin effects are marginal even at very high laser powers and/or electron energies, as anticipated in our heuristic analysis in Sec. I. On the other hand there are some interesting phenomena observable at very powerful laser fields that we shall discuss in more detail below.

### III. NUMERICAL EXAMPLES AND DISCUSSION

The following numerical analysis of the differential cross sections (9), (26), and (27) for a linearly polarized electromagnetic plane wave, leading to the generalized Bessel functions (13), was made possible by the work of Leubner [37] who has shown in his investigations how to efficiently evaluate these functions by using generalized saddle-point methods. His program developed for that purpose was modernized and adapted by us for our present problem. We shall fix

the screening length  $\ell$  of the scattering potential to  $\ell = 1$  a.u. and take for the nuclear charge  $Z = 1$ . As frequency of the radiation field we shall choose  $\omega = 1.17$  eV of a Nd:YAG laser. We investigate the angular and intensity dependence of the energy-conservation relation (10) and of the differential cross sections  $d\sigma_N/d\Omega'$ , given by Eqs. (9), (26), and (27) for selected values of the laser-field intensity  $I$ , initial kinetic electron energy  $E_{kin}$ , and order of nonlinearity  $N$ . As it turns out, it is of particular interest to consider high-energy electrons in the MeV range and, similarly, to choose radiation powers for which the ponderomotive energy  $U_p = m\mu^2/4$  is of the order of magnitude of the electron rest energy  $m$ .

We start with analyzing the energy-conservation relation (10) for the large value  $N = 10^3$  of absorbed photons at a laser power of the magnitude  $I = 1.28 \times 10^{18}$  W cm $^{-2}$  for which the parameter  $\mu$ , defined in Eq. (8), has the value  $\mu = 1$  and we take for the initial kinetic electron energy, before entering the laser beam,  $E_{kin} = 0.5m$ . The energy-conservation relation Eq. (10), written down for quantities considered outside the laser beam, can be presented in the form

$$E' = E - \frac{1}{4} m^2 \mu^2 \left( \frac{1}{E' - \mathbf{p}' \cdot \mathbf{n}} - \frac{1}{E - \mathbf{p} \cdot \mathbf{n}} \right) + N\omega, \quad (28)$$

where  $E' = m + E'_{kin}$  and  $E = m + E_{kin}$  are the relativistic energies of the scattered and ingoing electron, respectively. By choosing the laser beam to propagate in the  $x$  direction, i.e.,  $\mathbf{n} \parallel \mathbf{e}_x$ , we define the angles  $\theta$  and  $\theta'$  by the relations  $\mathbf{p} \cdot \mathbf{n} = \cos \theta$  and  $\mathbf{p}' \cdot \mathbf{n} = \cos \theta'$ , respectively. In Fig. 1 we present the corresponding dependence of the final kinetic energy  $E'_{kin}$  on the scattering geometry. In the upper left frame we show for the above parameter data a contour plot of the energy distribution  $E'_{kin}$  in the  $(\theta', \theta)$  plane and, for getting a better idea, we present in the frames, denoted by (a) and (b), the energy values along two cuts through this plot for fixed  $\theta'$ , namely, in (a) for  $\theta' = 20^\circ$  and in (b) for  $\theta' = 150^\circ$ , while in (c) the cut is made at the fixed value  $\theta = 20^\circ$ . These plots show very clearly the strong dependence of the final kinetic energy  $E'_{kin}$  on the angles of electron incidence and of scattering. The energies in these plots are presented in units of the electron's rest energy  $m$ . As can be clearly seen in plot (c), the final energy  $E'_{kin}$  has its smallest values where the outgoing electron moves in the direction of propagation  $\mathbf{n}$  of the laser beam. On the other hand, the largest kinetic energy gain is observed when the incoming electron moves parallel to the propagation direction.

In Figs. 2 and 3 we analyze the dependence of the differential cross sections, either evaluated from Eq. (9) for a Klein-Gordon particle or from Eqs. (26) and (27) for a Dirac particle. For presenting our data, we chose in both Figures, the laser beam to propagate along the  $x$  axis and its unit vector of linear polarization,  $\epsilon$ , to define the  $z$  direction, which also determines our polar axis whereas the azimuthal angle  $\varphi$  is measured with respect to the  $x$  axis in the  $(x, y)$  plane. Our results are shown for fixed polar angles of electron incidence  $(\theta, \varphi)$  and of scattering  $(\theta', \varphi')$  as a function

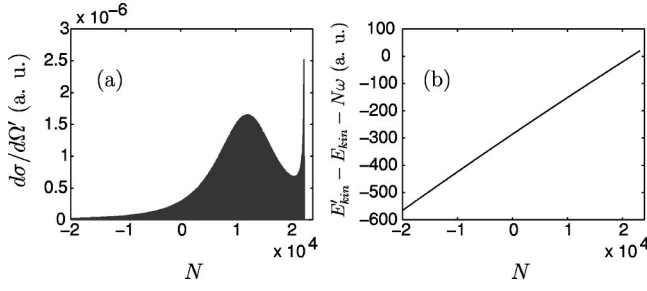


FIG. 2. Panel (a) presents the differential cross sections for the parameters  $I=10^{19}$  W cm $^{-2}$  and  $E_{kin}=2m$  as a function of  $N \leq 0$  for  $\theta'=1^\circ, \varphi'=0^\circ$  and electron incidence along  $\epsilon$ . The cross sections are large for  $N \gg 0$  and the cutoff is near  $N_0=22\,352$ . Panel (b) demonstrates the deviation of the relativistic energy-conservation law from the nonrelativistic one.

of the number  $N$  of absorbed or emitted laser photons  $\omega$ . Both relativistic cross-section formulas yield, in general, the same results. We shall discuss deviations between the data for a particle of spin 0 and spin 1/2 further below. As it turns out, the cross sections are particularly large for small scattering angles. Therefore the angles of electron incidence with respect to the  $z$  axis are chosen as  $\theta=0^\circ$  and  $\varphi=0^\circ$  and we consider scattering at a very small angle with  $\theta'=1^\circ$  and  $\varphi'=0^\circ$ . The laser frequency  $\omega$  will be the same as before but for the intensity we chose  $I=10^{19}$  W cm $^{-2}$  and for the initial kinetic electron energy we took  $E_{kin}=2m$ . In Fig. 2 we present the evaluated differential cross sections as a function of  $N$  in panel (a), which shows that these cross sections (presented in atomic units, denoted by a.u.) are considerably larger for photon absorption than for photon emission. A reasonable estimate for the cutoff value  $N_0$  of the electron spectrum can be found from the approximate formula  $N_0 = \pm|x| \pm 2|y|$ , where  $x$  and  $y$  are the two arguments of the generalized Bessel functions, Eq. (13). In our present case, the numerical calculations for the data shown in panel (a) yield the cutoff at  $N_0 \approx 22\,352$ . For this case, the arguments  $x$  and  $y$  are found to be  $x \approx -23\,238$  and  $y \approx 126$  so that  $|x| - 2|y| \approx 22\,986$ , which is in reasonable agreement with the value of  $N_0$  given before. In panel (b) we show the deviation of the relativistic energy-conservation law, Eq. (28), from the nonrelativistic energy relation  $E'_{kin} = E_{kin} + N\omega$ . This deviation represents an intensity-dependent energy excess. In Fig. 3 we present on an enlarged scale certain parts of the spec-

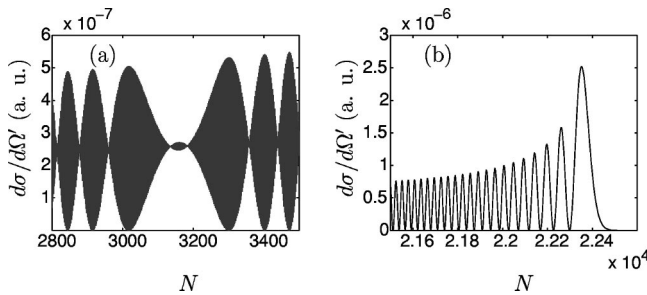


FIG. 3. On an enlarged scale, the behavior of the cross-section data of Fig. 2 in (a) in the vicinity of their maximum values and (b) near the cutoff at  $N_0$ .

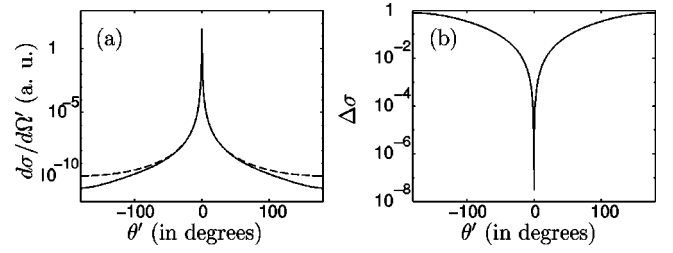


FIG. 4. Presents for the same scattering configuration and parameter values as in Fig. 2 and for elastic scattering, with  $N=0$ , in the left panel the differential cross sections of Mott scattering (solid line) and Klein-Gordon scattering (dashed line) as a function of  $\theta'$ . In the right panel is shown the normalized difference  $\Delta\sigma$  of these cross sections. Apparently, spin effects are visible only at large scattering angles.

trum shown in panel (a) of Fig. 2. In the left panel (a) we see on a larger scale, a section of the rising part of the spectrum for  $N > 0$  presented in panel (a) of Fig. 2, and we recognize that this spectrum is actually not smooth but shows rapid quasiperiodic oscillations. Similarly, we see in panel (b) the rapid oscillations of the data near the cutoff of the spectrum shown in panel (a) of Fig. 2. Summarizing, our results in Figs. 2 and 3 show that the cross-section data perform rapid oscillations as a function of the nonlinear order  $N$ . Such rapid changes with an almost periodic sequence of maxima and minima can be qualitatively well explained by analyzing the properties of the generalized Bessel functions  $B_N$  defined in Eqs. (13) and (14). This analysis, however, cannot be done analytically due to the complicated dependence of both arguments in Eq. (14), via Eq. (8), on the number  $N$  of emitted or absorbed photons, but requires a numerical evaluation. This result is very much different than the findings in nonrelativistic potential scattering in a laser field, since in the low-frequency limit the argument of the Bessel functions  $J_N$  in Eq. (15) becomes independent of  $N$ .

As we have indicated before, in the relativistic regime of electron kinetic energies  $E_{kin}$ , being of the same order of magnitude as the electron rest energy  $m$ , the scattering formulas for a Klein-Gordon particle and a Dirac particle yield almost the same cross-section values, in particular, for close to forward scattering where the cross-section data are largest. On the other hand, the expression (9) and Eqs. (26) and (27) yield significantly different values for the cross sections in the backward direction where, however, the cross-section values are particularly small. In order to show this, we present in panel (a) of Fig. 4 a comparison of the Klein-Gordon and Mott scattering data for the same scattering geometry as before, i.e., with electrons impinging on the target along the  $z$  axis ( $\theta=\varphi=0^\circ$ ) and scattered by an angle  $\theta' > 0^\circ$  for  $\varphi'=0^\circ$  or scattered by an angle  $\theta' < 0^\circ$  for  $\varphi'=180^\circ$ . The ingoing kinetic energy of the electron is  $E_{kin} = 1$  MeV  $\approx 2m$  and we consider the elastic case with  $N=0$ . As we recognize, the cross-section data (dashed line for Klein-Gordon particles and solid line for Dirac particles) are almost identical except for backward scattering. This can be seen even more clearly in panel (b) of Fig. 4 where we present the normalized difference  $\Delta\sigma$  of these cross-section data defined by

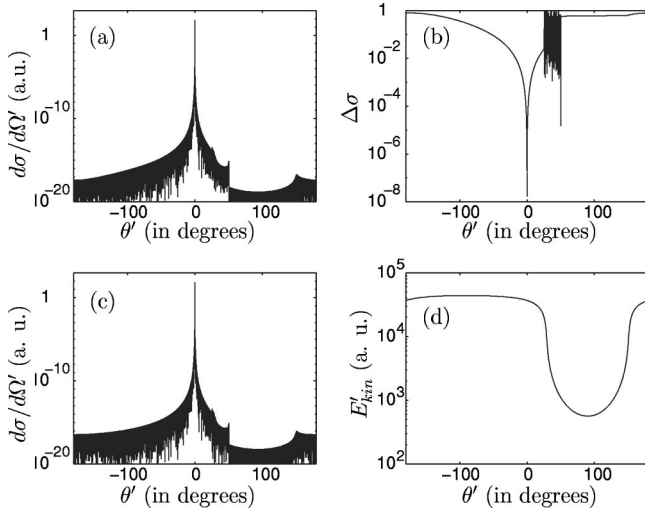


FIG. 5. Shows on a larger scale for  $N=0$  in panel (a) the spin-averaged cross sections of Mott scattering and in panel (c) the corresponding data for scattering of a spin-0 particle. In panel (b) we see the normalized differences  $\Delta\sigma$  of the data in (a) and (c). These differences are appreciable for large scattering angles but negligible for  $\theta'=0^\circ$ . In (d) we see that  $E'_{kin}$  can change significantly for large  $\theta'$ .

$$\Delta\sigma \equiv \frac{\left| \frac{d\sigma_D}{d\Omega} - \frac{d\sigma_{KG}}{d\Omega} \right|}{\frac{d\sigma_D}{d\Omega} + \frac{d\sigma_{KG}}{d\Omega}}, \quad (29)$$

which can have the values  $0 \leq \Delta\sigma \leq 1$ . As this panel shows, for  $|\theta'| \approx 0^\circ$  the deviations between the cross-section data for Dirac and Klein-Gordon particles are very small and only gradually increase for  $|\theta'|$  approaching backscattering at  $180^\circ$ .

In Fig. 5 we show a somewhat different presentation of the data evaluated for the previous figure. The scattering geometry and the parameter values are the same as in Fig. 4. In panel (a) and panel (c) we show, respectively, the differential cross sections evaluated for Mott scattering from Eq. (27), summed and averaged over the spin orientations, and for scattering of a Klein-Gordon particle calculated from Eq. (9). Almost no difference can be recognized between these two spectra. In panel (b) we show once more  $\Delta\sigma$  and we can only recognize a discrepancy between the data for a spin- $(1/2)$  and spin-0 particle at large scattering angles  $\theta'$ . At these large angles  $\theta'$  we also find that the final electron kinetic energy  $E'_{kin}$  has a considerable intensity and angular-dependent dip with a minimum value near  $\theta' \approx 90^\circ$ . This originates in the relativistic energy-conservation relation (28), as it implicitly shows this dependence on  $\theta$  and  $I$  since the ponderomotive energy  $U_p \sim I$ .

The properties of the differential cross sections, presented in the Figs. 4 and 5, can be found, in general, for values of  $N \neq 0$  and for relativistic electron energies and laser intensities where  $E_{kin}$  and  $U_p$  are in the MeV energy range. The differences between the cross sections for a Dirac and a

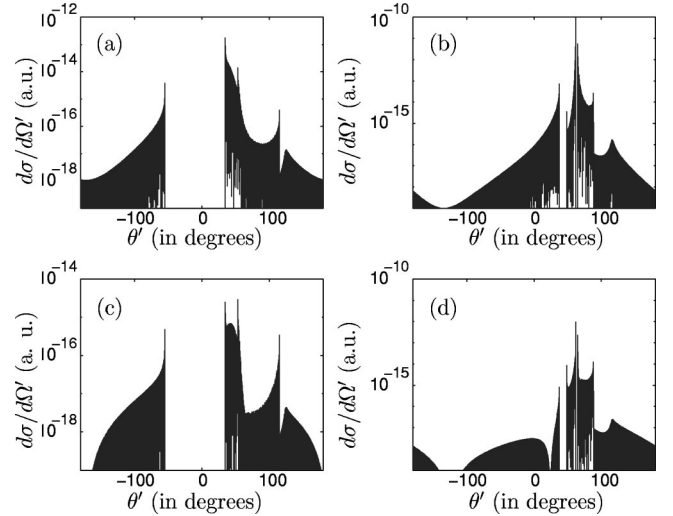


FIG. 6. In panels (a) and (c) are shown the cross-section data of Mott scattering for no spin flip and for spin flip, respectively, for electron incidence at  $\theta=0^\circ, \varphi=0^\circ$  and, correspondingly, the analogous data are found in (b) and (d) for  $\theta=50^\circ, \varphi=0^\circ$ . The data with spin flip are appreciably smaller than those without flip. Otherwise, the data in (a) and (c) and correspondingly in (b) and (d) show certain similarities as regards cross-sectional angular windows and peak structures.

Klein-Gordon particle will be significant only at large scattering angles where we shall simultaneously find a dip in the final electron energy  $E'_{kin}$ .

Finally, we investigate in some detail the dependence of the nonlinear cross sections for a Dirac particle on the spin orientation and spin flip. For the data presented in Fig. 6, we chose the same scattering geometry and parameter values as before and consider the absorption of a very large number of photons from the laser beam during the scattering, namely,  $N=10^6$ . The differential cross sections, evaluated from Eq. (26) for the spin orientations ( $s=+, s'=+$ ) and for ( $s=-, s'=-$ ), are identical and the same holds for the cross sections with spin flip ( $s=+, s'=-$ ) and ( $s=-, s'=+$ ). In panel (a) we present the data for  $d\sigma^{(+,+)}$  or, equivalently, for  $d\sigma^{(-,-)}$  for electron incidence in the forward direction at  $\theta=0^\circ, \varphi=0^\circ$  and, similarly, the same is shown in panel (c) for  $d\sigma^{(+,-)}$  or  $d\sigma^{(-,+)}$ . If we compare the data in these two panels, we recognize that spin flip leads to cross sections that are by about one order of magnitude smaller than the data for no flip and we also see differences in the angular behavior, except that the wide angular windows in which the cross sections vanish and some other structures of the spectra are similar. An analogous comparison is made between the cross-section data for electron incidence at  $\theta=50^\circ, \varphi=0^\circ$  in the panels (b) for no spin flip and (d) for flip. Here too the cross sections for spin flip are smaller than those for no flip and the angular windows are at the same positions in (b) and (d) but the detailed structure of the spectra is different. We may therefore conclude that the probabilities of changing the spin orientation during scattering are, in general, very much smaller than for no change of the spin orientation, at least for the highly relativistic electron energies and laser intensities considered.



#### IV. SUMMARY AND CONCLUSIONS

In the present work we have investigated the potential scattering of relativistic electrons in a very powerful, linearly polarized laser field. The scattering process was described at these energies by the first-order Born approximation and, for comparison, we represented the electron, embedded in the electromagnetic plane-wave field, either as a particle of spin 0, using the Gordon solution [29], or as a particle of spin 1/2, employing the Volkov solution [28]. In both cases the relativistic energy-conservation relation in the laser field is the same but it now depends on the initial and final electron momenta and on the laser power. As our numerical analysis has shown, the spin effects on the differential cross sections  $d\sigma_N/d\Omega'$  with the emission or absorption of  $N$  laser photons are, in general, marginal in the present process, in particular, for scattering in the close to forward direction. Small spin effects by spin flip can be observed at large scattering angles where, however, the cross sections are very small. Even in this case, the data with spin flip are by orders of magnitude smaller than those with no flip. In this latter case the cross sections for a Dirac particle are almost identical with those for a Klein-Gordon particle over the whole

range of scattering angles. Of particular interest, as in our previous investigations of this scattering problem at lower laser-field intensities, is a scattering configuration in which the electrons impinge on the target in the direction of the laser polarization  $\epsilon$  and the scattering plane is determined by the direction of propagation  $\mathbf{n}$  of the laser field and its polarization  $\epsilon$ . We expect on the basis of the results of our investigation for laser powers (measured by the ponderomotive energy) and for electron energies in the MeV range, being equivalent to energies of the electron's rest mass, that similar conclusions can also be drawn for other fundamental scattering processes, namely, that spin effects are, in general, marginal for laser-induced or laser-assisted processes even at very high laser powers. Such investigations we intend to perform in our forthcoming work.

#### ACKNOWLEDGMENTS

This work was supported by the Scientific-Technical Collaboration Agreement between Austria and Poland for 2000-01 under Project No. 2/2000. One of the authors (P.P.) acknowledges the partial support by the Polish Committee for Scientific Research (Grant No. KBN 2 P03B 039 19).

- 
- [1] J.H. Eberly, in *Progress in Optics*, edited by E. Wolf (North-Holland, Amsterdam, 1969), Vol. VII, and references therein.
  - [2] F.B. Bunkin, A.E. Kazakov, and M.V. Fedorov, *Usp. Fiz. Nauk.* **107**, 559 (1972) [*Sov. Phys. Usp.* **15**, 416 (1973)].
  - [3] M.H. Mittleman, *Introduction to the Theory of Laser-Atom Interactions*, 2nd ed. (Plenum, New York, 1993).
  - [4] F.H.M. Faisal, *Theory of Multiphoton Processes* (Plenum, New York, 1987).
  - [5] C.J. Joachain, M. Dörr, and N. Kylstra, *Adv. At., Mol., Opt. Phys.* **42**, 225 (2000).
  - [6] P. Francken and C.J. Joachain, *J. Opt. Soc. Am. B* **7**, 554 (1990).
  - [7] F. Ehlötzky, A. Jaroń, and J.Z. Kamiński, *Phys. Rep.* **297**, 63 (1998).
  - [8] F.H.M. Faisal, *Radiat. Eff. Defects Solids* **122-123**, 27 (1991).
  - [9] H.R. Reiss, *Prog. Quantum Electron.* **16**, 1 (1992).
  - [10] D.D. Meyerhofer, *IEEE J. Quantum Electron.* **33**, 1935 (1997), and references therein.
  - [11] M. Protopapas, C.K. Keitel, and P. Knight, *Rep. Prog. Phys.* **60**, 389 (1997), and references therein.
  - [12] C. Szymanowski, V. Vénard, R. Taïeb, A. Maquet, and C.H. Keitel, *Phys. Rev. A* **56**, 3846 (1997), and references therein.
  - [13] M.M. Denisov and M.V. Fedorov, *Zh. Éksp. Teor. Fiz.* **53** 1340 (1940) [*Sov. Phys. JETP* **26**, 779 (1968)].
  - [14] H. Brehme, *Phys. Rev. C* **3**, 837 (1971).
  - [15] L. Schlessinger and J. Wright, *Phys. Rev. A* **20**, 1934 (1979).
  - [16] J. Bergou and S. Varró, *J. Phys. A* **13**, 2823 (1980).
  - [17] D.B. Milošević and P.S. Krstić, *J. Phys. B* **21**, L303 (1988).
  - [18] P.S. Krstić and D.B. Milošević, *Phys. Rev. A* **39**, 1783 (1989).
  - [19] D-S. Guo and T. Åberg, *J. Phys. B* **24**, 349 (1991).
  - [20] F.H.M. Faisal and T. Radożycki, *Phys. Rev. A* **47**, 4464 (1993).
  - [21] L. Rosenberg, *Phys. Rev. A* **33**, 164 (1986).
  - [22] J.Z. Kamiński, *J. Phys. A* **18**, 3365 (1985).
  - [23] L. Rosenberg and F. Zhou, *J. Phys. A* **24**, 631 (1991).
  - [24] F. Zhou and L. Rosenberg, *Phys. Rev. A* **45**, 7818 (1992).
  - [25] F. Morales, G. Ferrante, and R. Daniele, *Nuovo Cimento D* **19**, 23 (1997).
  - [26] F.V. Bunkin and M.V. Fedorov, *Zh.Éksp. Teor. Fiz.* **49**,1215 (1966) [*Sov. Phys. JETP* **22**, 844 (1966)].
  - [27] N.M. Kroll and K.M. Watson, *Phys. Rev. A* **8**, 804 (1973).
  - [28] D.V. Volkov, *Z. Phys.* **94**, 250 (1935).
  - [29] W. Gordon, *Z. Phys.* **40**, 117 (1926).
  - [30] J.Z. Kamiński and F. Ehlötzky, *Phys. Rev. A* **59**, 2105 (1999).
  - [31] P. Panek, J.Z. Kamiński, and F. Ehlötzky, *Can. J. Phys.* **77**, 591 (2000).
  - [32] J.Z. Kamiński, P. Panek, and F. Ehlötzky, *Laser Phys.* **10**, 163 (2000).
  - [33] F. Ehlötzky, *Nuovo Cimento Soc. Ital. Fis., B* **69**, 73 (1970); *Opt. Commun.* **27**, 65 (1978).
  - [34] L. I. Schiff, *Quantum Mechanics*, 3rd ed. (McGraw-Hill, New York, 1968), p. 478, Eq. (52.25).
  - [35] H. Prakash and N. Chandra, *Nuovo Cimento Soc. Ital. Fis., B* **55**, 404 (1968).
  - [36] L.S. Brown and T.W.B. Kibble, *Phys. Rev.* **133**, A705 (1964).
  - [37] C. Leubner, *Phys. Rev. A* **23**, 2877 (1981).